JOURNAL OF MATERIALS SCIENCE **36** (2001) 4167–4180

The effect of material defects on the fatigue behaviour and the fracture strain of ABS

R. MARISSEN*‡
DSM Research, P.O. Box 18, 6160 MD Geleen, The Netherlands; Delft University of Technology, The Netherlands
E-mail: roelof.marissen@dsm.com

D. SCHUDY, A. V. J. M. KEMP, S. M. H. COOLEN, W. G. DUIJZINGS, A. VAN DER POL, A. J. VAN GULICK
DSM Research, P.O. Box 18, 6160 MD Geleen, The Netherlands

The structural integrity and durability of a construction are highly dependent on the material quality. Poly(Acrylonitrile-Butadiene-Styrene) Copolymer (ABS) is a material which is preferably chosen for high performance products, because of its superior toughness. The toughness of ABS is revealed by its high fracture strain in a tensile test, and high notched Izod impact fracture energy. However, the fatigue resistance of ABS is less favourable. This investigation is mainly devoted to the fatigue behaviour of ABS and to the fracture strain and the notched Izod fracture energy. Various mechanical tests, performed in conjunction with scanning electron microscope investigations of the fracture surfaces, demonstrate that fracture initiates from small defects which are abundantly present in the material. Especially the fatigue fracture surfaces show numerous cracks which had initiated from the defects. The fracture strain in tensile tests is high, but shows a large scatter. It is demonstrated that the fracture strain is also related to the presence of defects. A pre-fatigue load up to 40% of the anticipated fatigue life, followed by a tension test shows a significant reduction of the fracture strain as compared with a tension test on non damaged as-moulded material. Microscopic investigations show that this fracture strain reduction is caused by the presence of small cracks which initiated from the defects, during the preceding fatigue load. A similar but much smaller effect of pre-fatigue was observed for notched Izod tests. Finally it is concluded that the fatigue behaviour of ABS is dominated by the growth live of microscopic small cracks from material defects.

1. Introduction

Fatigue resistance of construction materials is highly important for long term integrity. Fatigue is the fracture of a material due to cyclic loading, where each load is smaller than the static strength of the material. However, fracture of materials may also occur due to so called static fatigue. Creep rupture, or stress rupture may be a less confusing name for that failure process. Fatigue is used exclusively for the cyclic fracture process in this paper. A convenient way of measuring and presenting fatigue properties of a material is through a so called S-N curve. Such a curve presents the critical stress level as a function of the number of load cycles to be sustained. A true S-N curve, without a creep rupture contribution, should be independent of the cyclic loading frequency. Independence of the fatigue life on the frequency is not necessarily expected, because polymers like ABS generally show time dependent mechanical behaviour. The negligibility of a contribution of creep rupture to the fracture process should be checked, before such a process is described as a "true fatigue" fracture.

The material quality with respect to fatigue can be measured and presented in diagrams with the aid of S-N curves. However, such representation hardly gives any explanation of the fatigue process. Additional post mortem investigations of the fracture surfaces may provide such explanation. The Scanning Electron Microscope (SEM) being a powerful apparatus for such fractographic investigations has been used extensively in this investigation, to explain the fatigue process. It was found that the presence of defects in the material is a very important contribution to the fracture process. Some additional investigations of the fracture surface are performed, using Raman microscopy. A new Raman imaging technique has been applied to the fracture surfaces. The Raman imaging technique revealed a clear difference between the chemical constitution of the defects and the surrounding material.

* Author to whom all correspondence should be addressed.
‡ *Present Address*: DSM High Performance Fibres, Eisterweg 3, NL-6422 PN Heerlen, The Netherlands.

Figure 1 The specimen for tensile and fatigue tests.

Tensile tests and notched Izod tests were performed to supplement the fatigue tests. These tests are performed in a conventional way, but they are also performed on pre-fatigued specimens. SEM fractograpy has also been used in these test series, on fracture surfaces resulting from the tests.

2. Material and specimens

A commercially produced ABS with code MAGNUM 3504 (Trademark of Dow Chemical Co.) was injection moulded into dogbone tensile specimens. This is a natural ABS type without pigments or fillers. The specimens were injection moulded through a film gate at one side. The specimen is shown in Fig. 1. The cross section in the measuring area is 4×10 mm. The length of the central measuring area is 50 mm.

Some notched Izod specimens were prepared, by cutting them from the central area of the tensile specimens.

3. Experiments

Stress strain curves were obtained by drawing the specimens in a Zwick 1455 testing machine. Most specimens were drawn at a rate of 10 mm/minute, while some other specimens were drawn at 180 mm/minute. The latter tests were performed to observe possible rate effects, and to obtain a loading rate more or less comparable to the loading rates applied in the fatigue experiments.

Fatigue tests were performed with a Schenk closed loop servohydraulic testing machine. The tests were performed with sinusoidal load variation in time, and a stress ratio $R = S_{\min}/S_{\max} = 0.1$. The maximum fatigue stress, $S_{\max}$, for the first fatigue test was fixed at 90% of the tensile strength of the tests with a drawing rate of 180 mm/minute. The fatigue life, being the number of load cycles up to fracture (in two separate pieces), was obtained from this test. Subsequently, tests with lower stress levels were performed. The number of cycles to fracture is obtained from these tests. A test frequency of 5 Hz has been chosen for most of the fatigue tests. Some tests with a frequency of 1 Hz were performed as well, in order to observe any possible frequency effect on the fatigue life. Fatigue test frequencies above 5 Hz were not selected, in view of possible heating up of the specimens due to hysteresis. A too large temperature increase of the polymer may change the material properties and the fatigue behaviour, as stated e.g. in [1]. Fatigue crack growth measurements on ABS [2] suggest that hysteresis heating is not a problem up to frequencies of 10 Hz. The chosen frequency of 5 Hz is therefore on the safe side. Indeed, no indications have been observed for a significant temperature increase in the present tests at 5 Hz.

Some fatigue tests were performed at 65% of the tensile strength in a constant strain rate test (180 mm/minute), but discontinued at 40% or 66% of the anticipated fatigue life (which was measured first on other specimens). These pre-fatigued specimens were then subjected to tensile tests at a drawing rate of 10 mm/minute. Pre-fatigued specimens with elapsed 66% of the fatigue life were also machined into notched Izod specimens. The resulting values of the notched Izod tests are compared with values obtained from specimens which were machined from non damaged (as moulded) tensile specimens.

4. Results of mechanical tests

The results of the tensile tests at a drawing rate of 10 mm/minute are presented in Fig. 2a–c. Note that the scale of Fig. 2a–c is identical. It is clearly observed that pre-fatigue has a significant effect on the fracture strain as measured. Another observation is that all curves in Fig. 2a have about the same shape. Only the strains at break, where the curves end are different. There is a significant scatter in fracture strain. The tensile curves in Fig. 2b reveal a similar shape again, but with an earlier end of the curves and also with a significant scatter of the fracture strain. This trend proceeds further in Fig. 2c with an even larger decrease in fracture strain. One specimen in Fig. 2c even failed before displaying a load drop. Pre-fatigue obviously causes a severe embrittlement in tensile tests.

The effect of the drawing rate is presented in the Table I. An increasing drawing rate causes an increasing maximum stress and a decreasing fracture strain. This result is not unexpected for a viscoelastic polymer, such as ABS.

The results of the notched Izod tests on as moulded (non damaged) and on pre-fatigued specimens are

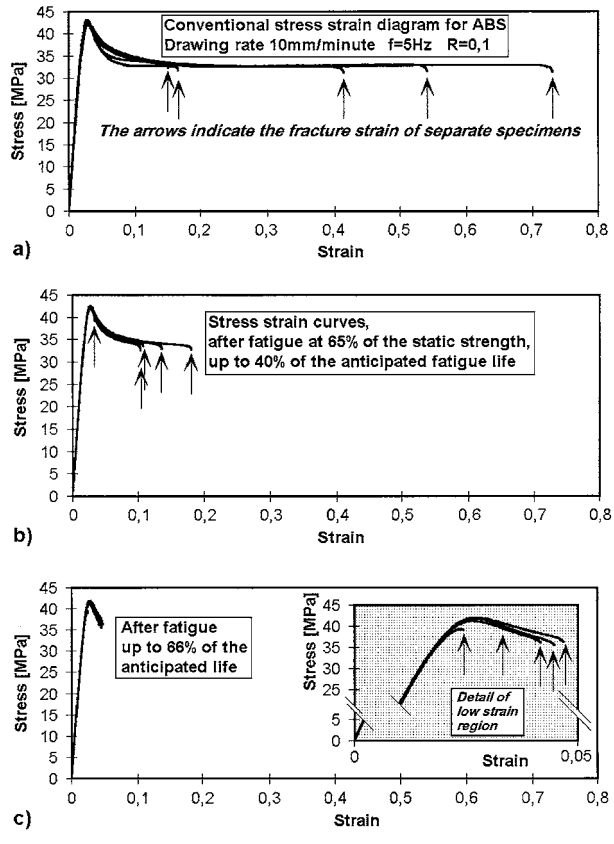

Figure 2 Tensile test results on as moulded, and on pre fatigued ABS specimens.

TABLE I The effect of the drawing rate on the yield stress and fracture strain of ABS tensile specimens

Drawing rate (mm/minute)	Average yield stress (MPa)	Average fracture strain
10	43	0.4
180	47	0.12

TABLE II Notched Izod test results for normal and for pre-fatigued ABS material

Conventional notched Izod test (kJ/m^2)	Notched Izod after pre-fatigue at 65% of static strength, up to 66% of the anticipated fatigue life (kJ/m^2)
28.03	25.08
27.84	26.10
28.24	27.19
27.77	25.32
27.20	23.76
Average value 27.82	Average value 25.49

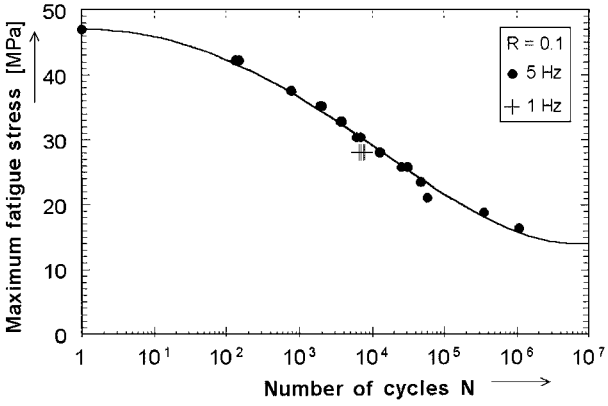

Figure 3 The S-N curve of ABS.

presented in Table II. It can be observed from Table II that the notched Izod tests reveal only a very slight but statistically significant embrittlement (scatter bands do not overlap) due to the pre-fatigue load.

The results of the fatigue tests are presented as an S-N curve in Fig. 3. The tensile strength, obtained from the tensile tests at 180 mm/minute is added to the figure as a strength at a fatigue life of one cycle. It may be considered as an asymptotic value in the S-N curve. It can be observed that ABS is rather sensitive to fatigue. About 1/3 of the static strength is available, if one million cycles have to be sustained. The S-N curve is still decreasing in the high cycle fatigue region around a million of cycles. It can also be observed that the fatigue life at a test frequency of 1 Hz is about half of the fatigue life observed at 5 Hz. If damage were due to time effects only and not due to cycling, a factor of 5 would be observed. Obviously, the damaging effect of cycling is larger than the damaging effect of time. Nevertheless, the effect of time is significant. In fact, this observation can also be discussed in terms of strength at the same fatigue life. The effect in terms of strength is similar to that of the tensile tests: fast loading is related to higher strength levels.

5. Fractography and discussion

The results presented above will be explained, using extensive Scanning Electron Microscope (SEM) investigations of the fracture surfaces. Fig. 4 shows a typical fractograph of a specimen fatigued at 65% of the tensile strength in a constant strain ratio test. The fracture surface is very faceted. Some of the facets have a parabolic shape. A magnification is presented in Fig. 5. It reveals the facets more clearly. A further magnification in Fig. 6 shows a pattern of "rays", emanating from the centre of the facets. Fig. 7 is a magnification of two facets, showing a location with a quite different morphology at the centre of the facet. A further magnification is presented in Fig. 8, showing that all rays emanate from a kind of particle with a size of about 15 microns. Obviously, the particle is a defect from which the fracture initiates. The fractographs in Figs 4–8 are typical for fatigue load levels of about 50% to 60% of the static strength. A typical size of the observed defects is 15 to 50 microns. So numerous facets are present on the fatigue fracture surface. All facets are microcracks starting from small defects. Obviously, the defects are abundantly present in ABS. Figs 9 and 10 reveal the fracture surface of a specimen which was fatigued at a stress of only 45% of the static strength. This low stress level appears to generate a few large facets only (one in Fig. 9). Again the facet shows a central particle. The morphology of the particle is different here, and the size is much larger as compared with the previous figures. The size of the defect in Fig. 10 is about 150 microns. The presence of a defect in the centre of a facet or in the "focal point" of a parabolic structure is found to be typical. Defects can be observed in the centre of all facets at sufficient magnification. Low fatigue stresses are obviously not able to initiate cracks from small defects. Only large defects are effective at low stresses. This explains the reduced amount of facets and the larger size of defects found on the fracture surface of specimens subjected to low fatigue stresses.

Inclusions in materials may act as stress concentrations if the deformation properties are different from the surrounding material. A different Young's modulus, Poisson's contraction, or yield stress may cause this effect. Also a lack of adhesion to the surrounding material may cause stress concentrations. A different Young's modulus can cause the largest stress concentrations. A low stiffness (Young's modulus) causes additional stresses in the surrounding material near the equator of the inclusion. A high stiffness inclusion causes higher stresses at the poles. The defect shown in Fig. 8 exhibits the most frequently observed morphology. It appears to be highly deformed in the centre, obviously it is a soft material, fractured in the middle. Indeed, a quite similar defect morphology was observed at the other fracture half, showing the other half of the defect particle. This type of defect appears to be rich on butadiene, as shown with RAMAN microscopy in the last part of this paper. Butadiene is the softest part of ABS, so the chemical constitution is consistent to the observed fracture surface morphology. On the other hand, the defect presented in Fig. 10 apparently shows its pole, so it appears to have been effective as the result of a larger stiffness

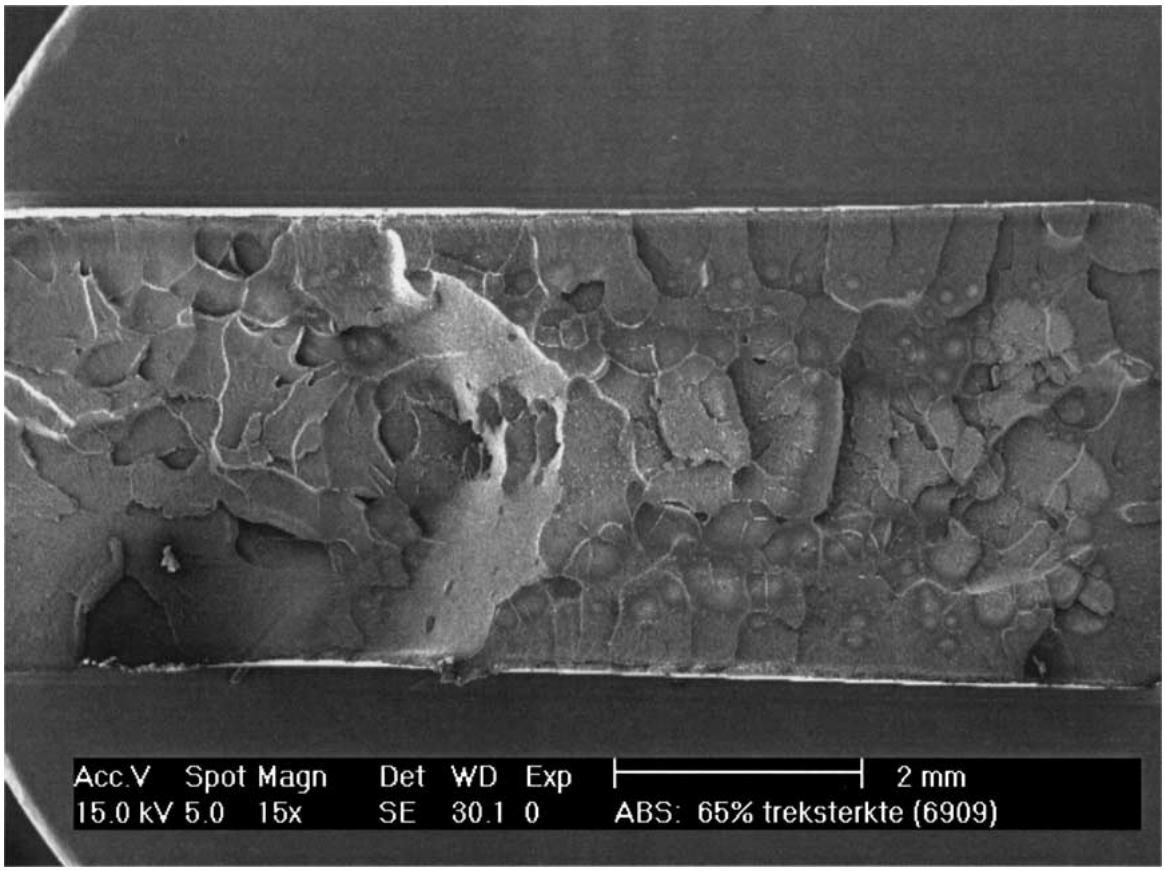

Figure 4 SEM micrograph of the fracture surface of a specimen, fatigued at 65% of the static tensile strength.

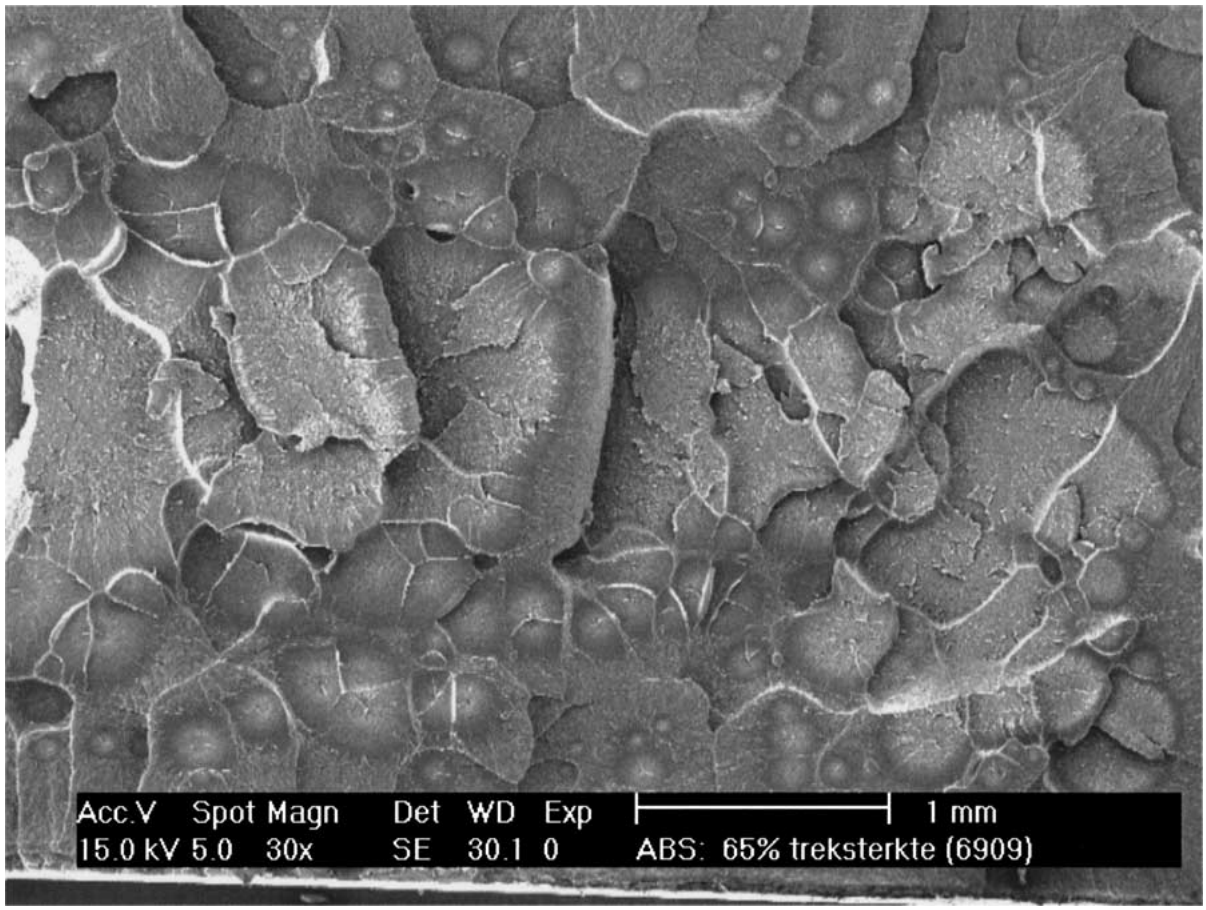

Figure 5 Magnification of the right-hand side of Fig. 4.

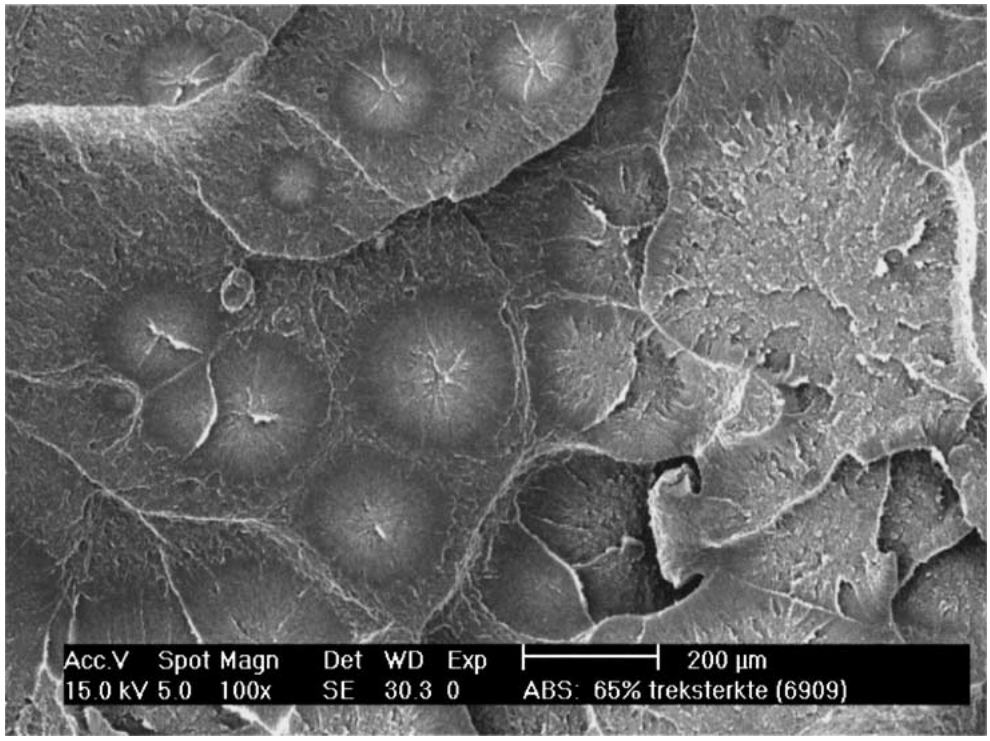

Figure 6 Further magnification of the upper right-hand side of Fig. 5.

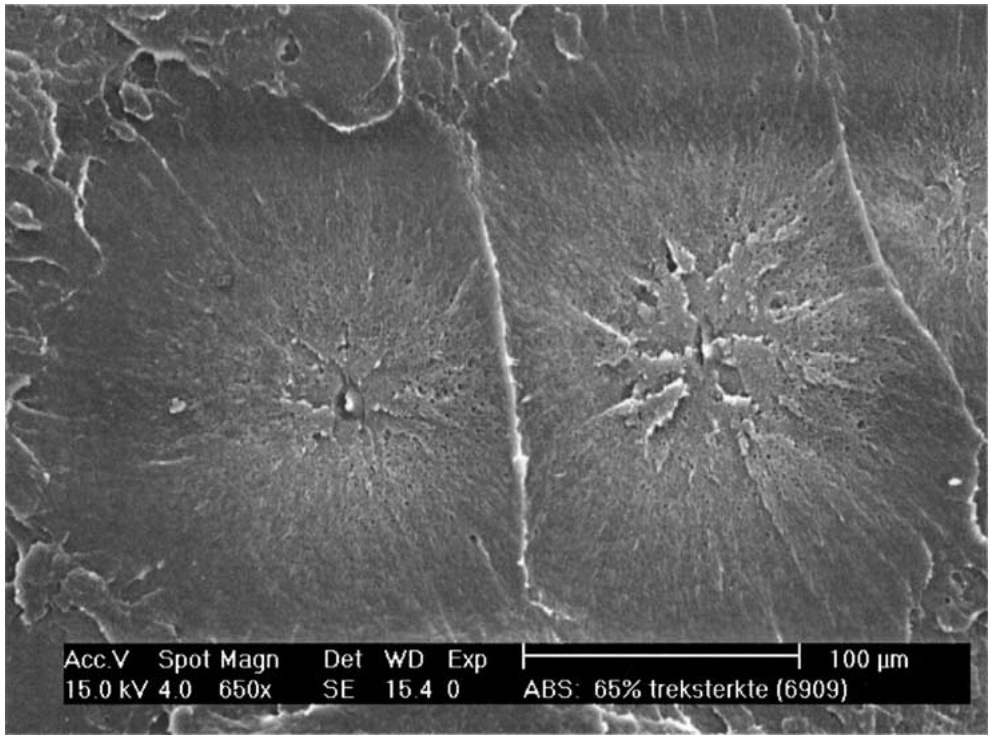

Figure 7 Magnification of two facets on the fracture surface.

and/or lack of adhesion to the surrounding material. A further discussion on fracture surface appearance, defects and some literature evidence is presented below.

Faceted fracture surfaces are typical for ABS. They have been presented in many papers. Examples can be found in [3–5]. However, magnifications are generally small and the micrographs are hardly discussed in detail. Discussions in terms of defects are even more rare. An exception is [5], showing a fractograph, and discussing it in terms of an observed defect indeed. However, no papers were found, indicating that fracture in ABS commonly initiates from internal defects. An interesting observation is reported in [6]. Although internal defects are not considered in [6], it demonstrates the sensitivity of ABS to small defects. The effect of electroplating on the fracture strain is investigated. Thin electroplating layers of about 20 micron in thickness, on ABS, reduce the fracture strain of the composite to about 4%. The authors show micrographs of crack initiation from the thin brittle electroplating layer, growing

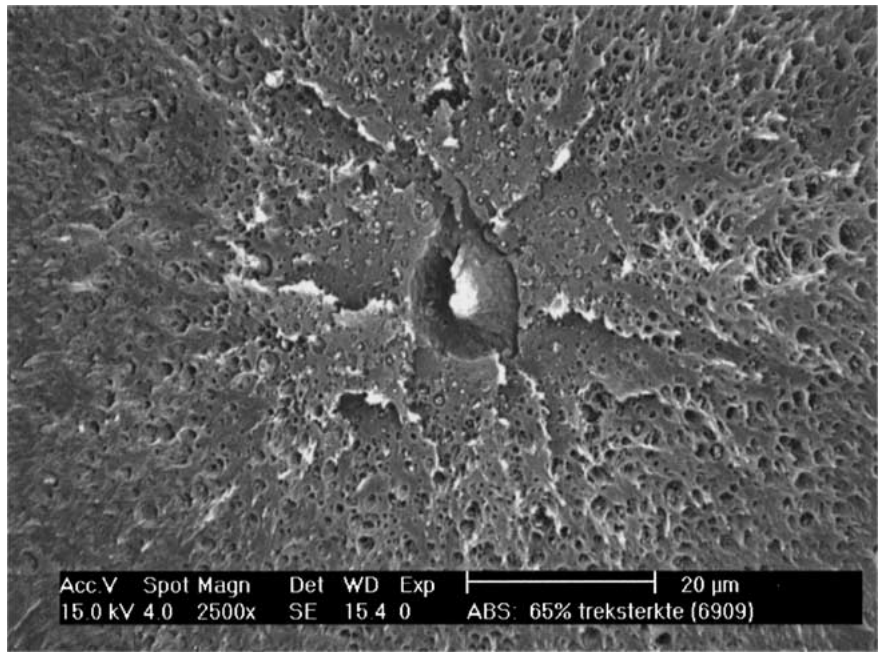

Figure 8 Further magnification of the centre of the left-hand facet in Fig. 7. The central defect is clearly visible.

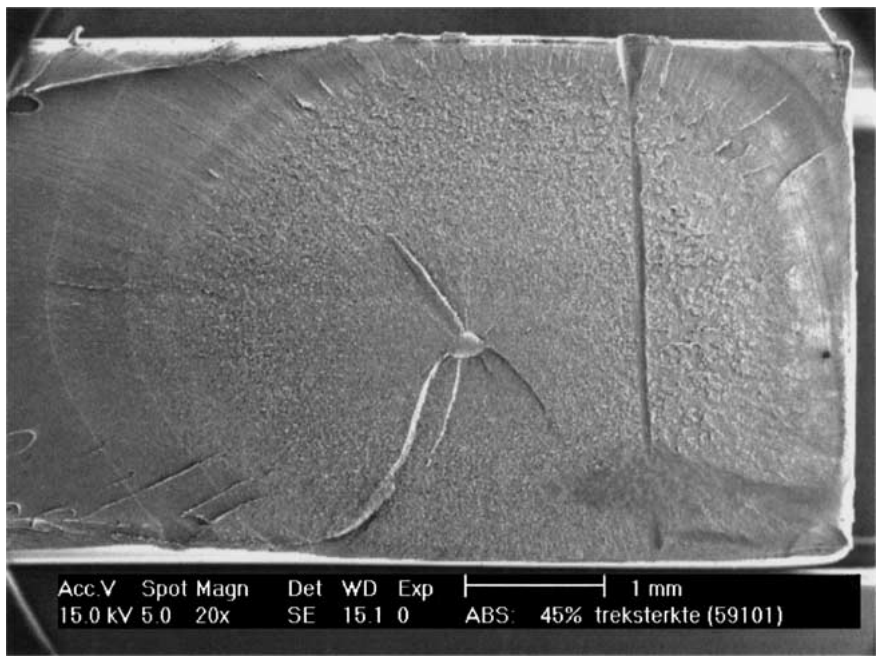

Figure 9 SEM micrograph of a fracture surface after fatigue at 45% of the static strength.

into the ABS substrate. Obviously, the thin electroplating layer acts as a defect, similar to the defects in the present investigation and a similar embrittlement is observed as caused by the presently described defects, especially for the pre-fatigue experiments in the present investigation. This confirms that ABS is already sensitive for defects with a size of about 20 microns. An example with a similar observation for surface coating of another polymer is given in [7]. Parabolic structures on the fracture surface have been observed before for other polymers. They have been explained by the growth of smaller collinear (coplanar) cracks or crazes, e.g. in [8]. Indeed, a small crack growing towards a faster growing (larger) crack will cause a parabolic marker on the fracture surface. This process is illustrated schematically in Fig. 11. The explanation in Fig. 11 postulates the start of a crack or craze at a defect. Larger defects will cause larger cracks, which will show higher growth rates. The smaller defect will be associated with the smaller crack, which will grow around the defect as a focal point within the parabolic surface of the smaller crack. Fig. 11 also illustrates that the closed side of the parabola (boundary of the surface of the smaller crack) is directed towards the direction of the opposing larger crack. It is easily understood, that if the number of defects and associated cracks is large, the parabolas will degenerate to facets, with borders to other cracks in all directions. Obviously the facets are related to micro cracks, and the particles are defects from which those cracks initiate. The fracture surface gives no direct

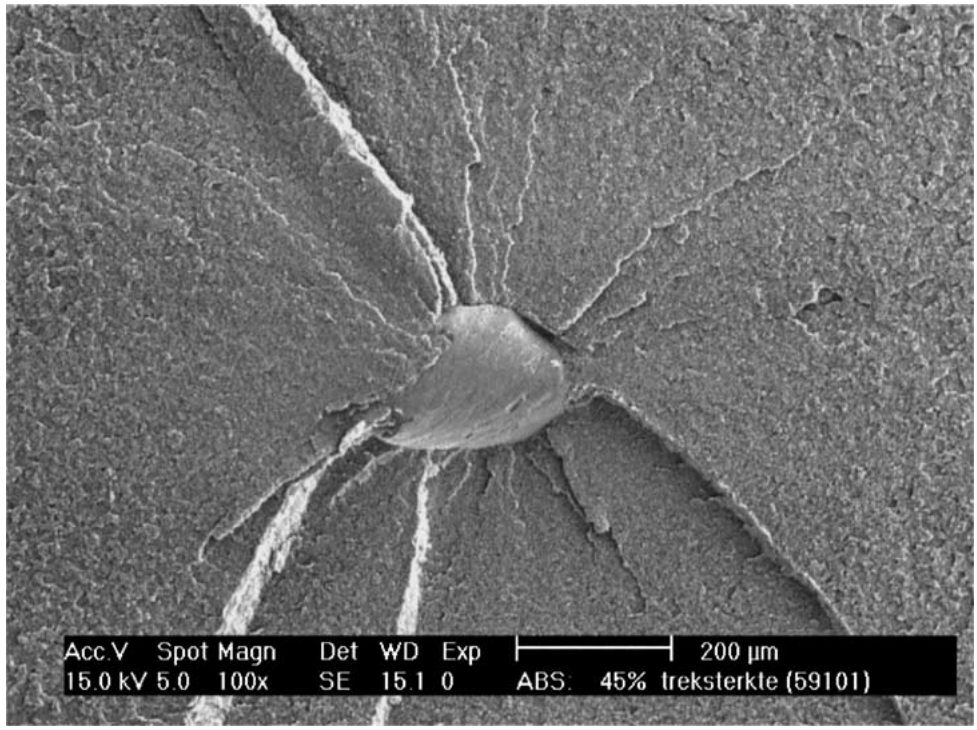

Figure 10 Further magnification of the centre of Fig. 9.

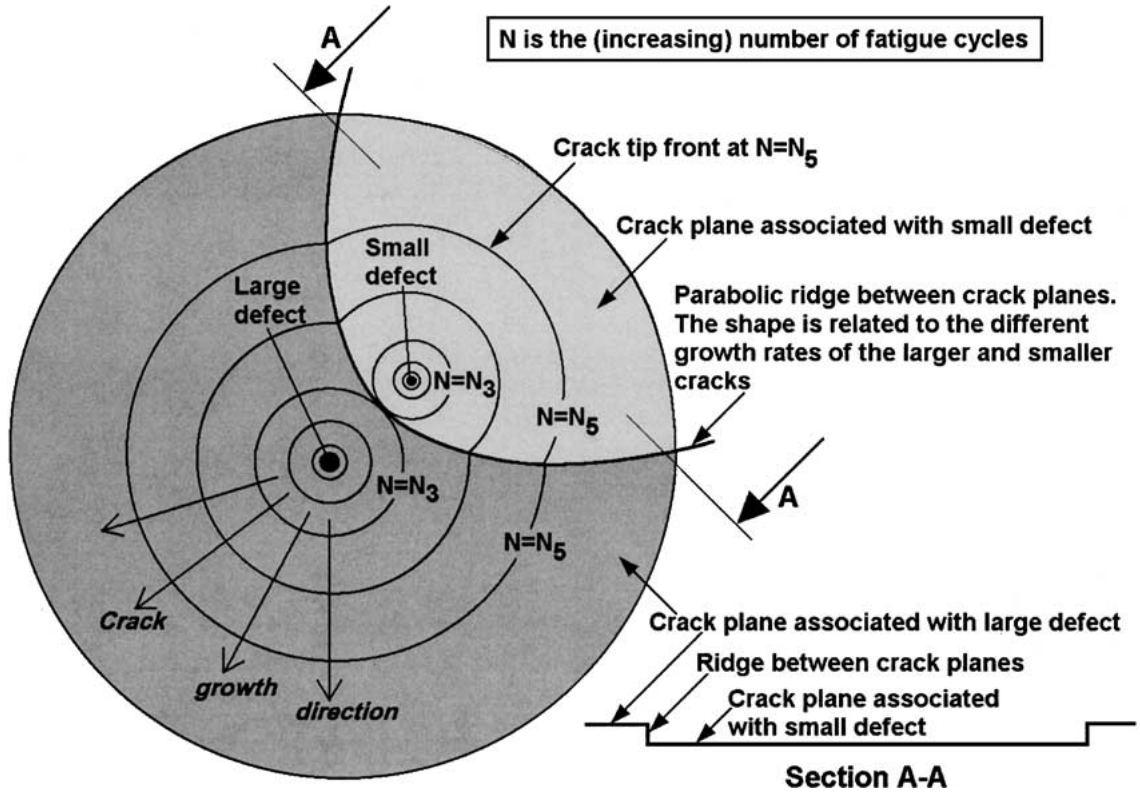

Figure 11 Schematic description of the formation of parabolic facets on the fracture surface.

indication whether cracks or crazes are to be adopted, or perhaps cracks with a tip craze. This will be discussed later. So far, the designation crack will be adopted. Obviously, the proposed fracture scenario of cracks starting from defects, is consistent with the observations on the fracture surface. ABS contains many of those defects. Similar defects as observed in this investigation have been observed by the present authors in many other polymers. However, the abundance as observed in ABS is rare. It is somewhat surprising that the significance of defects got only limited attention in previous publications. One reason may be that fatigue tests as performed in the present investigation allow easier interpretation of fracture surfaces. Defects are postulated in another paper of a present author [9]. That paper presents a fracture mechanics based theoretical prediction of craze growth rates in PVC, for crazes growing from defects. The observations in the present paper

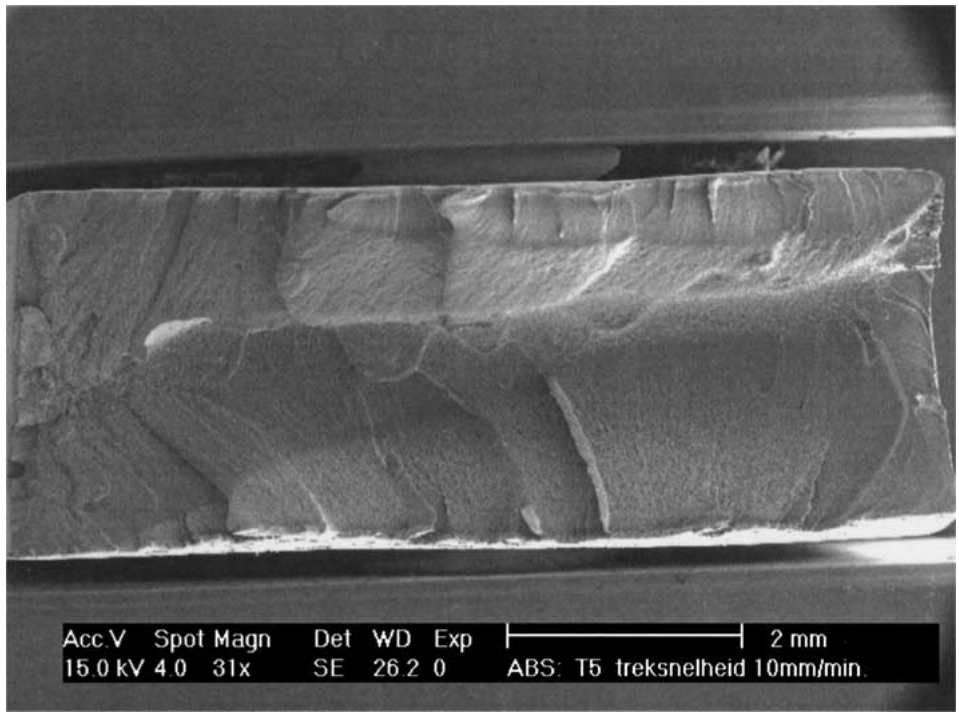

Figure 12 SEM micrograph of the fracture surface of a static tensile test at 10 mm/minute.

provide an additional motivation for the defects postulated in the model for craze growth in PVC. Some other publications, indicating the importance of defects in polymers are discussed below.

The time to failure under creep rupture conditions has been measured in [10] for polyethylene (PE). Creep rupture and fatigue fracture are both subcritical fracture processes, so some similarity may be expected. The use of different filters during melt processing of the polymer was investigated [10]. Course filters allow the presence of large defects in the material. Fine filters remove large defects and allow the presence of small defects only. The longest stress rupture lifetimes were obtained with finer filters, obviously because larger defects were filtered away and because large defects cause early initiation of cracks. The effect of filters explained with the effect of defect size is consistent to the present observations. Addition of aluminium powder to the material in [10] caused the presence of even larger defects. The time needed for rupture was found to be even smaller for the material containing the larger aluminium particles. Again, this behaviour is rather similar as found in the present investigation. Consequently, a rather general conclusion may be that the fracture behaviour of polymers is influenced to a considerable extent by the presence of micro defects and the polymers resistance against crack or craze initiation from these defects and the resistance against the growth of these cracks or crazes. Fracture surfaces, showing such defects in PE, and explaining it consistently with the arguments above have been presented in [11]. Fracture surfaces of PVC have been presented in [12, 13], showing some parabolas and facets, indicating the presence of defects. The so called diamond cracks in PVC described in [14] may quite well be explained as cracks, which have just started from a defect. In view of the preceding discussion, the parallel planes of the diamond may be considered to be the defect, whereas the inclined areas are crack flanks connected at the crack tip at the diamond edge. SEM fracture surfaces with very clear parabolas and some facets have been presented in [15]. However, the magnifications are insufficient to detect the defects and the authors do not mention them. Nevertheless, the very typical pictures, including "rays" emanating from the focal points of the parabolas, indicate that the investigated polymer contained many defects from which cracks initiated. Numerous fracture surfaces have been presented in [16]. Many of them show defects and are discussed in terms of defects. However, Figures 258 and 259 in [16] show an ABS fracture surface similar to those presented in the present investigation. The centre of the facet was designated as the initial craze. However, in view of the evidence of the present investigation, discussed before and below, it must be concluded that it was a defect instead of an initial craze.

The SEM micrographs of the fracture surfaces of samples broken in constant strain rate tests are presented in the Figs 12–14. Again, the fracture surfaces have a facetted appearance, although the number of facets is smaller than for most of the fatigue specimens. A new feature in the fractographs from the tensile tests is that the specimen surface now appears to have a defect character. Some faint parabolas are observed in Fig. 12. The closed side of these faint parabolas are always pointing towards the specimen surface. Considering that the parabolas direct their closed side towards the advancing larger crack (as discussed before), it must be concluded from Fig. 12 that the main crack growth occurs from the surface towards the specimen centre. Some facets are found in the centre region of the fracture surface. SEM micrography in Figs 13 and 14 reveals again defects in the centre of these facets, although they are far more difficult to recognise than in

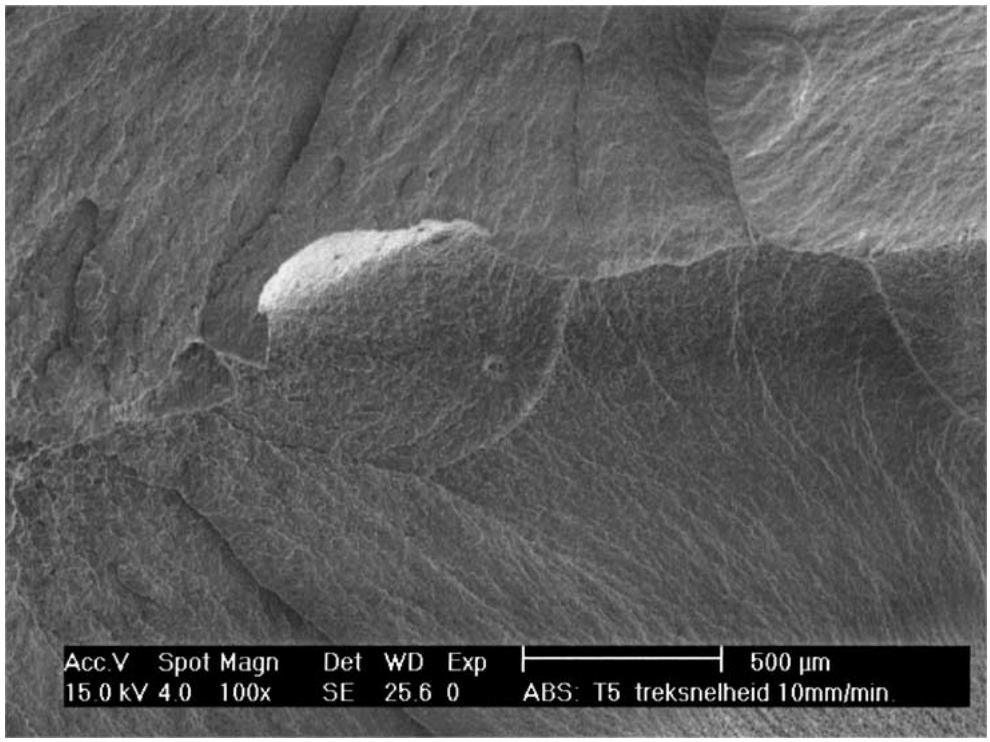

Figure 13 Magnifigation of the left-hand part of Fig. 12.

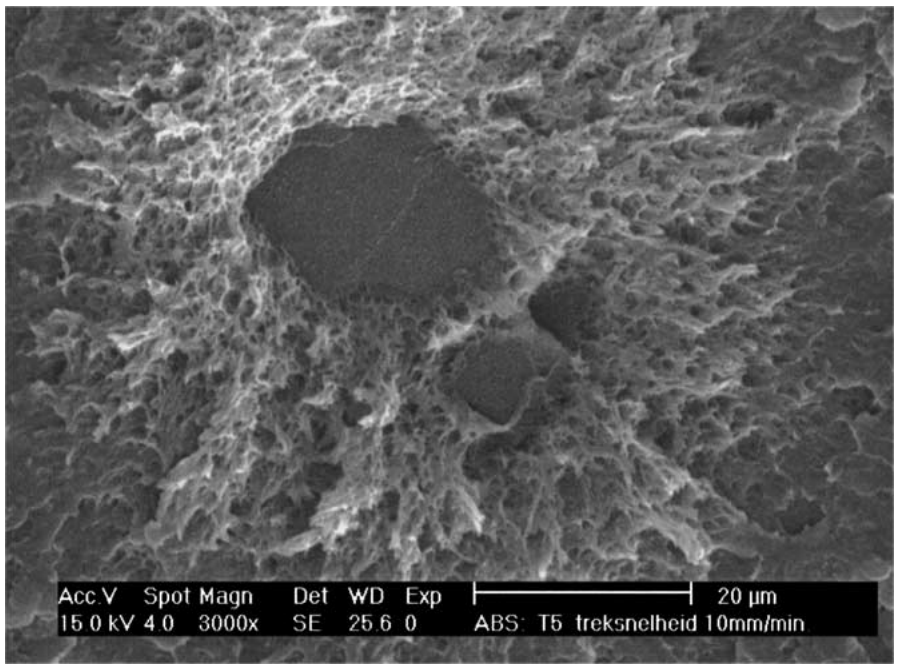

Figure 14 Magnification of the central part of the facet in Fig. 13.

the fatigue fracture surfaces. The more difficult recognition explains why the defect character of the centre of the facets or focal point of the parabolas has hardly been discussed in the literature. Yet, considering the large similarity with the easily interpreted fatigue fracture surfaces, the fracture scenario of cracks emanating from defects should be adopted to be similar. In fact, a gradual change of the fracture surface morphology towards that of the monotonic tensile tests is observed for fatigue tests at higher stress levels. The amount of facets is also decreasing for larger fatigue stresses. Obviously not only a sufficiently large stress is needed to initiate large numbers of cracks, as discussed before for the high cycle fatigue range, but also a sufficient number of cycles is important. The lower number of fatigue cycles at higher stresses obviously reduces the number of initiated cracks. The extreme situation is the "one cycle" tensile test, activating the initiation of a few cracks from a few defects only. Another reason is the competition with the defect character of the surface. This may be explained by surface orientation during injection moulding. Oriented surfaces will have a somewhat higher yield stress, but a lower fracture strain. The lower fracture strain is insignificant in the fatigue tests which

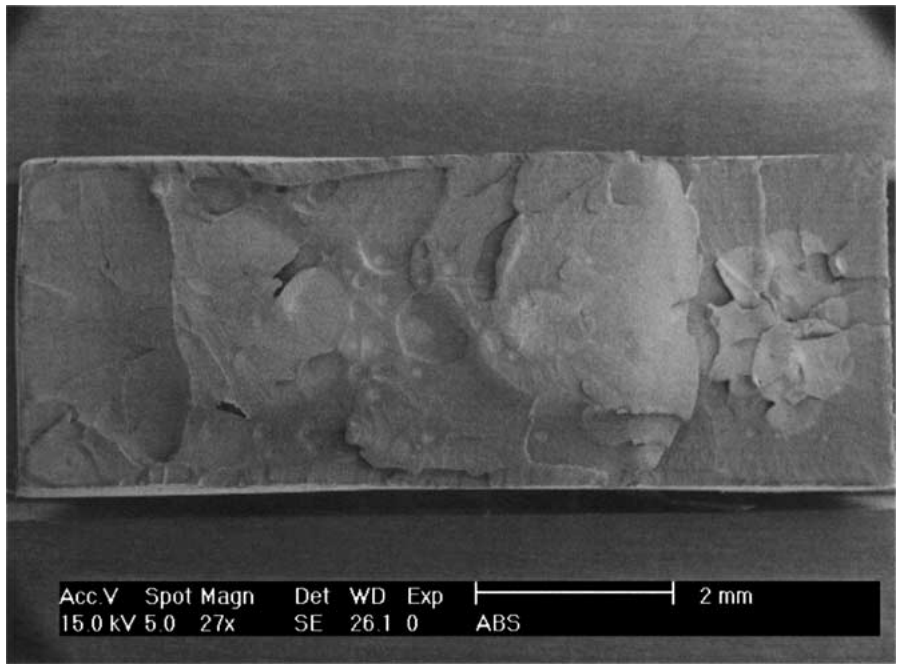

Figure 15 Micrograph of a specimen, loaded in fatigue at 65% of the static strength, up to 40% of the anticipated fatigue life, and subsequently subjected to a static tensile test. The fracture strain was 10%.

show a low strain anyhow. But it may cause earlier cracking in a monotonic tensile test. Anyhow, the SEM micrographs indicate that the defect particles are also important for the fracture behaviour in the static tensile test. Fig. 2 indicates that there is only one parameter to be influenced: the fracture strain! The observed scatter in the fracture strains can now be explained by the very local character of the fracture process. Fracture indeed occurs at the tip of the cracks, initiated from defects. On the other hand, the shape of the stress strain curve is a consequence of global material behaviour, it is a material property and not influenced by defects. The defects determine to which strain up to fracture the intrinsic stress-strain curve is followed.

The stress strain curves in Fig. 2b and c support the above argument. Fatigue up to 40% of the anticipated fatigue life, (from Fig. 3) already causes some crack initiation and crack growth. These micro cracks act as large defects and cause a reduction of the fracture strain in the subsequent tensile test. Again, with a similar shape of the stress strain curve. The SEM micrograph of Fig. 15 actually shows those fatigue cracks as small circles on the fracture surface. Further magnification in the area of the circles shows the same typical features as discussed before for pure fatigue fracture surfaces (therefore not presented here). The micrograph in Fig. 15 is obtained from the specimen in Fig. 2b, which showed a fracture strain of 10%. Fig. 2c indicates that pre-fatigue up to 66% of the anticipated fatigue life causes an even more reduced fracture strain in the subsequent tensile test. This is of course related to even larger fatigue cracks. It can be concluded that for fatigue cycling of ABS at 65% of the static strength, at least 60% of the fatigue life is spent during growth of micro cracks. Considering that the cracks in Fig. 15 will have spent some cycles, for growing up to the observed size, and that growth rates of small cracks are small, the portion of the fatigue life spent during growth of micro cracks might even be significantly longer than 60% of the fatigue life.

A similar but much smaller effect of a fatigue preload was found for the result of the notched Izod tests. Indeed, an observation of the fracture surfaces in the Figs 16 and 17 reveal small circular micro cracks on the fracture surface of the pre-fatigued notched Izod specimens. Some accompanying parabolic features around the circles are also observed. The fracture surfaces of the conventional notched Izod tests are presented in Figs 18 and 19. They also show parabolas, but now associated with a defect at the focal point. A striking difference with the fracture surface of the pre-fatigued notched Izod specimens is the complete absence of facets. Indeed, the facets are fatigue microcracks which initiated and grew during the fatigue load, which preceded the notched Izod test. Obviously, defects and micro cracks are also relevant for the notched Izod tests. However, regarding the limited effect on the measured notched Izod fracture energy, the relevance is much smaller than for the tensile tests. The notch itself is the largest defect and it dominates the fracture process. The notch also determines the location of the fracture. This is important for the pre-fatigued specimens, because only fatigue micro cracks being present at the notch location contribute to the fracture. So, only cracks in a very small volume of material are important for the notched Izod test result. The situation in the tensile test of course is totally different. The largest micro crack in the entire measuring volume of the specimen will dominate the fracture process. This explains the large embrittlement due to pre-fatigue in the tensile tests and the small embrittlement effect in the notched Izod tests.

The matter of crazes or cracks was raised before. It is well known that craze fibrils are easily damaged during the unloading part of a fatigue cycle, Fracture of the damaged craze fibrils will cause the craze to become a true crack. This is one reason for adopting

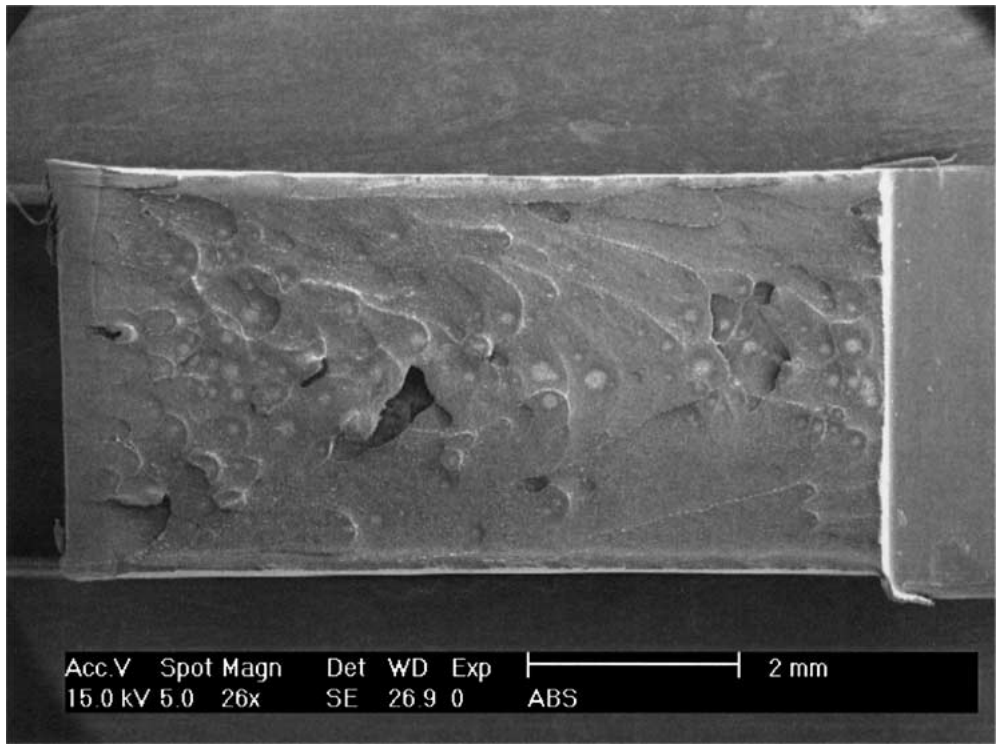

Figure 16 Micrograph of a specimen, loaded in fatigue at 65% of the static strength, up to 66% of the anticipated fatigue life, and subsequently subjected to a notched Izod test. The notch area is visible at the right side. So crack growth is from right to left.

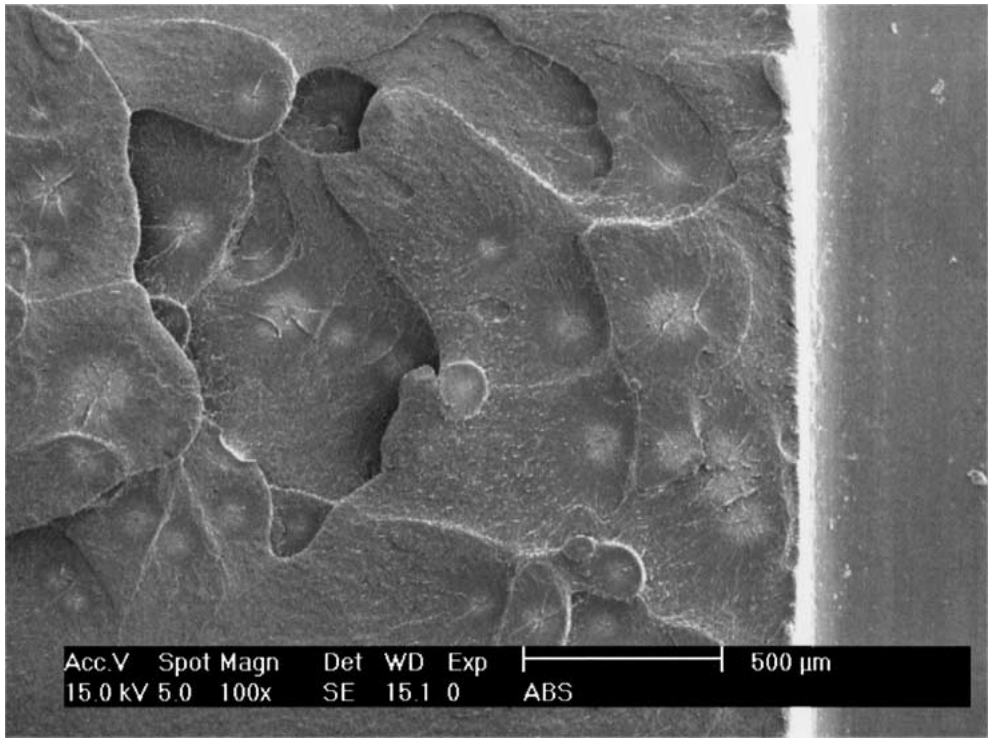

Figure 17 Detail of Fig. 16.

the scenario of cracks initiating from defects. ABS is a material which develops many crazes during plastic straining. Adding some crazes during a pre-fatigue load would add a hardly significant effect to the fracture process and the fracture strain would hardly be influenced. Consequently, in view of the embrittlement observed in Fig. 2b and c, it must be concluded that something more severe than a craze was developed. This leaves the adoption of the crack scenario as the only plausible possibility. The abundant presence of defects in ABS and the growth of damage from these defects has been demonstrated convincingly. The defects are important for the fatigue strength and the fracture strain of ABS, and to a much lesser extent also for the notched Izod tests.

A final part of fractographic evidence has been obtained with imaging Raman microscopy. The Raman imaging technique has been described in another publication [17]. Fig. 20 shows a part of the Raman spectrum of ABS. The spectrum shows peaks due to the presence

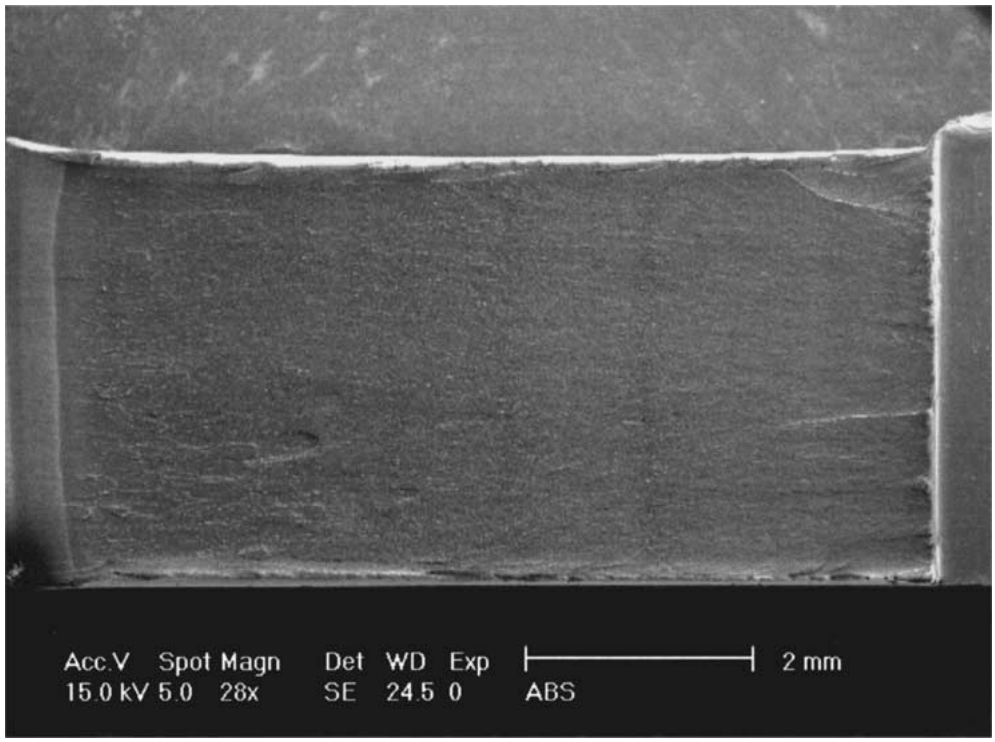

Figure 18 Micrograph of a specimen subjected to a conventional notched Izod test.

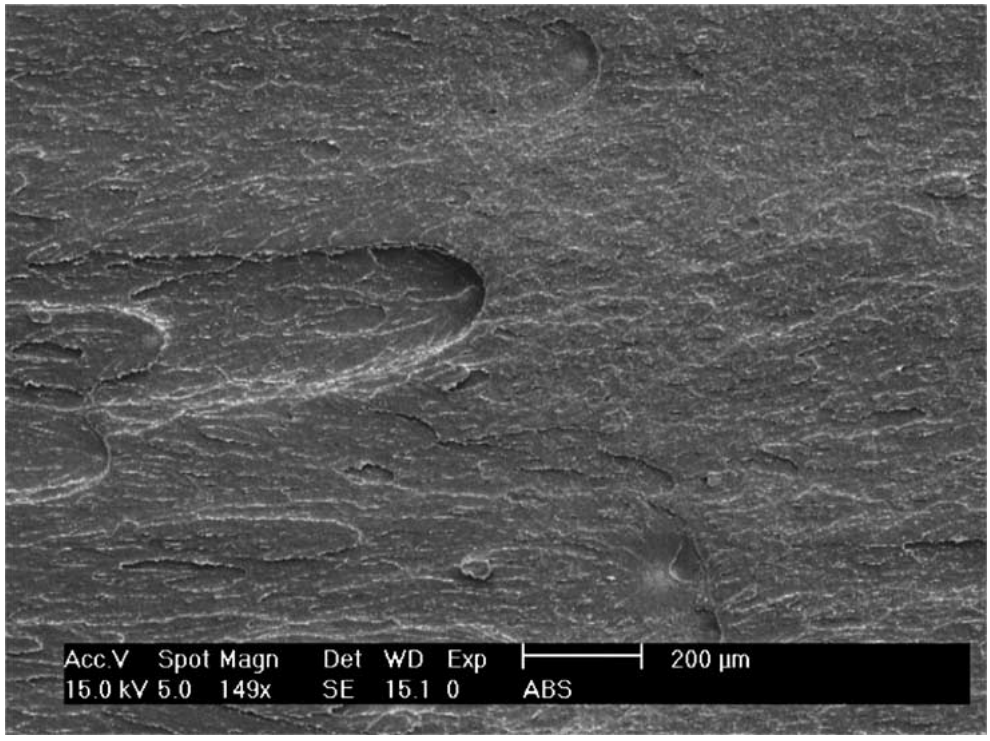

Figure 19 Detail of Fig. 18.

of styrene (aromatic C−H bending) denoted as S, butadiene (C=C stretch) denoted as B, and acrylonitrile (C≡N stretch) denoted as A. A part of a fracture surface containing a defect was scanned. Raman spectra were recorded for every square of 5×5 microns. The ratio of the peak areas for each square is calculated and presented as a grey scale in an image of the fracture surface. The counterpart of the fracture surface shown in Fig. 21 has been used for this Raman imaging procedure. The Figs 22–24 show the images of the peak ratios A/S, B/A and B/S respectively. An elementary image processing programme is used to flip the image to a similar position as Fig. 21. It is very clear that the defect region shows a different chemical constitution. Moreover, a concentric structure is revealed. A rather large area of about 100 microns exists, which is rich in acrylonitrile and butadiene. Within that area, a smaller core is visible which is especially rich in butadiene. The size of the core is about 30 microns. The core size is the same as that of the central particle visible with SEM

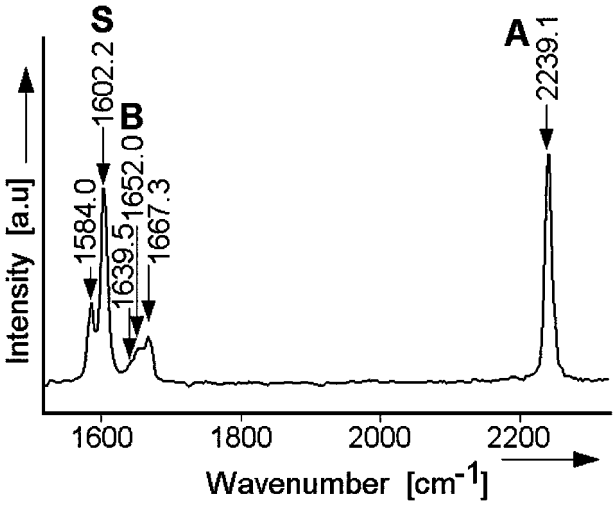

Figure 20 A part of the Raman spectrum of ABS, showing signals due to styrene, butadiene and acrylonitril.

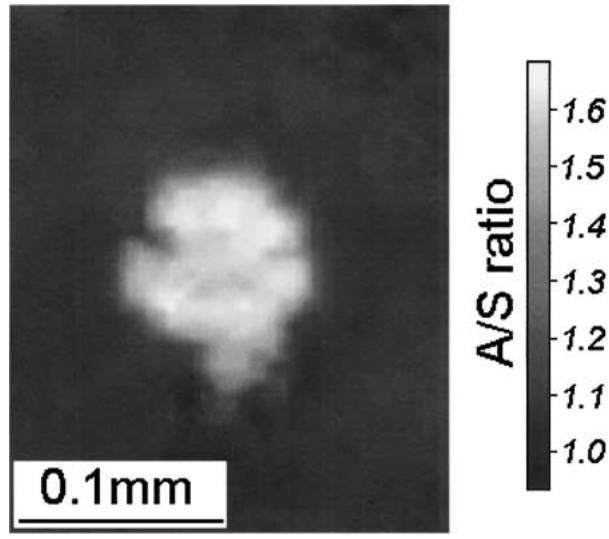

Figure 22 A Raman image of the A/S peak ratio, of a part of the fracture surface with a defect.

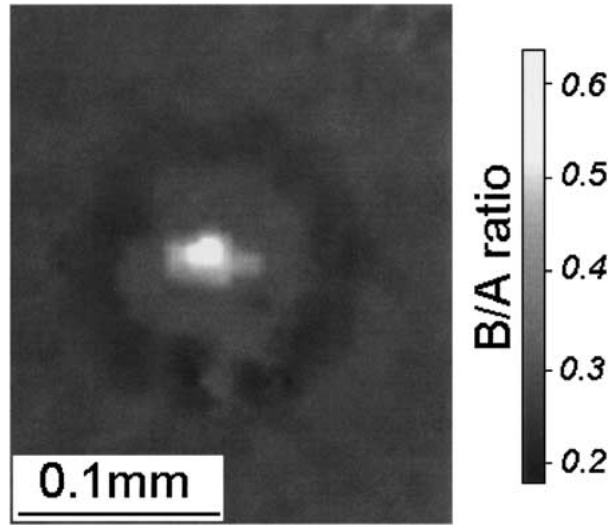

Figure 23 A Raman image of the B/A peak ratio, of a part of the fracture surface with a defect.

as presented in Fig. 21. Moreover, even the shapes of the defects in Figs 21 and 24 are similar. Obviously, the butadiene rich core is the actual defect in a mechanical sense. Fig. 21 also reveals a slight indication for a different morphology of the fracture surface over about 100 microns. However, obviously only the core area with relatively much butadiene acts as a defect. This is consistent with the fracture morphology of the defects. Many of them they show a kind of highly drawn morphology in the middle. Figs 8 and 21 are examples. Obviously the defects consist of material with a low glass temperature and low stiffness, as should be expected from butadiene rich material. A low stiffness material causes high stresses in the surrounding material near the equator of the defect as discussed before.

ABS is a so-called reactor blend, very small butadiene particles with a size of about 0.2 microns are present as a rubbery toughening constituent. However, also much larger butadiene rich particles of up to 50 microns appear to occur. These larger particles obviously

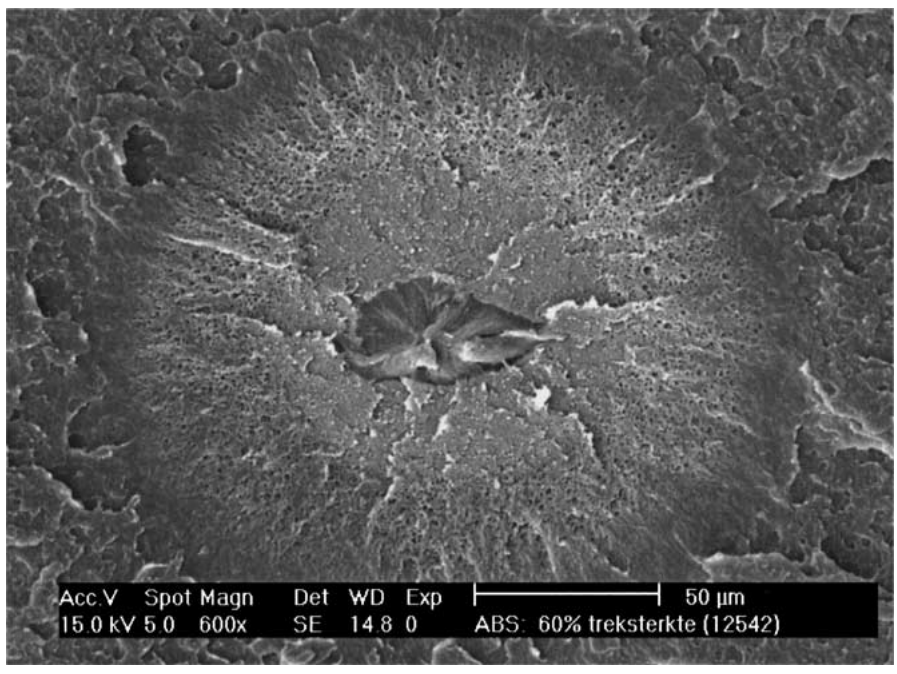

Figure 21 A defect in a fatigue specimen loaded at 60% of the static strength. It is the opposite position of Figs 22–24, on the other fracture half.

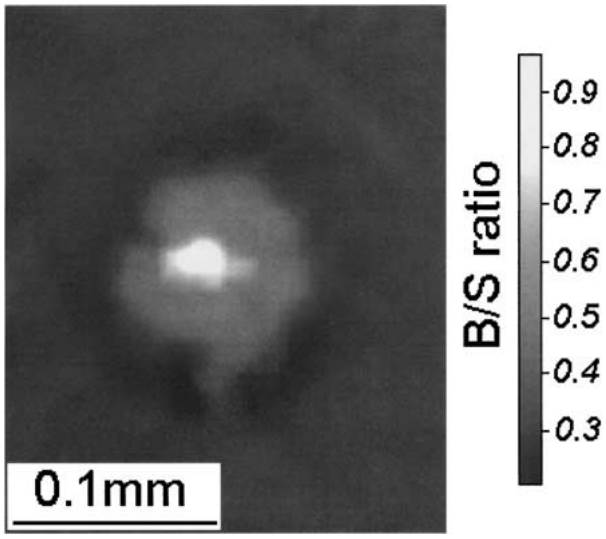

Figure 24 A Raman image of the B/S peak ratio, of a part of the fracture surface with a defect.

act as defects and they initiate fracture. The origin of the large particles was not a part of the present investigation. However, considering that rubber toughening of ABS is established in the reactor, and considering the abundant occurrence of the defects, and the very reproducible morphology of most of the defects, including the surroundings, it is probable that the defects arise already during the synthesis of the polymer.

Summarising, it can be stated that the defects are indeed particles with a constitution, being different from that of the surrounding material. The particles are rich on butadiene. Butadiene is the rubbery constituent of ABS. However, instead of micron or submicron rubbery particles, the defects are up to 50 micron "large" soft particles. Indeed, such soft particles will represent defects in a mechanical sense and may quite well be able to initiate the cracks observed on the fracture surface.

6. Conclusions

The fatigue behaviour of ABS has been investigated. Additional tensile tests and notched Izod tests have been performed. The effect of pre-fatigue load on the tensile and notched Izod tests was established. It was observed that:

1. ABS is sensitive to fatigue
2. A limited effect of the fatigue frequency was observed
3. An abundant amount of defects is present in ABS
4. The defects influence the fatigue life and the fracture strain of ABS
5. The effect of defects on the notched Izod test result is small
6. Fatigue cracks initiate and grow, already in an early stage of the fatigue life. Most of the fatigue life may be spent during the growth of micro cracks
7. Micro cracks generated during a fatigue load up to 40% of the anticipated fatigue life, cause a significant embrittlement in a subsequent tensile test.
8. An embrittlement effect of fatigue micro cracks on the notched Izod test result is present, but it is small
9. The chemical constitution of the defects is different from that of the surrounding material

References

1. R. W. LANG, M. T. HAHN, R. W. HERTZBERG and J. A. MANSON, *J. Mater. Sci. Lett.* **3** (1984) 224.
2. H. S. KIM and X. M. WANG, *J. Appl. Polym. Sci.* **57** (1995) 811.
3. J. A. SAUER and C. C. CHEN, *Pol. Eng. Sci.* **24**(10) (1984) 786.
4. C. B. BUCKNALL and W. W. STEVENS, Proceedings of the Int. Conf. Toughening of Plastics, Plast. Rubber Inst. London (1978) p. 24.1.
5. J. A. SAUER and C. C. CHEN, in "Crazing in Polymers," edited by H. H. Kausch (Springer-Verlag, Berlin, Heidelberg, New York, Tokyo, 1983) p. 170.
6. M. MATSUNAGA and Y. HAGIUDA, *Metal Finishing* (1971) 36.
7. M. BOSMA, Ph.D. Thesis, Delft University of Technology, 1994.
8. D. HULL, in "Polymeric Materials," edited by E. Baer and S. V. Radcliffe (Metals Park, OH, 1975) p. 487.
9. R. MARISSEN, *Polymer* **41** (2000) 1119.
10. G. SANDILANDS, P. KALMAN, J. BOWMAN and M. BEVIS, *Polymer Communications* **24** (1983) 273.
11. M. B. BARKER, J. BOWMAN and M. BEVIS, *J. Mater. Sci.* **18** (1983) 1095.
12. J. BREEN, *ibid.* **29** (1994) 39.
13. J. BREEN and D. J. VAN DIJK, *ibid.* **26** (1991) 5212.
14. P. L. CORNES and R. N. HAWARD, *Polymer* **15** (1974) 149.
15. WEN-BING LIU and FENG-CHIH CHANG, *J. Appl. Polym. Sci.* **56** (1995) 545.
16. L. ENGEL, H. KLINGELE, G. EHRENSTEIN and H. SCHAPER, "Scanning Electron Microscope Investigations of Damage in Plastics" (in German) (Carl Hanser Verlag München, Wien, 1978).
17. L. MARKWORT and B. KIP, *J. Appl. Polym. Sci.* **61** (1996) 231.

Received 11 July 2000
and accepted 19 April 2001